Comparison of Transcranial Focused Ultrasound and Transcranial Pulse Stimulation for Neuromodulation: A Computational Study

Dennis Q. Truong, PhD[1]; **Chris Thomas, BE**[1]; **Benjamin M. Hampstead, PhD**[2,3]; **Abhishek Datta, PhD**[1,4]

ABSTRACT

Objective: The objective of the study was to investigate transcranial wave propagation through two low-intensity focused ultrasound (LIFU)–based brain stimulation techniques—transcranial focused ultrasound stimulation (tFUS) and transcranial pulse stimulation (TPS). Although tFUS involves delivering long trains of acoustic pulses, the newly introduced TPS delivers ultrashort (~3 μs) pulses repeated at 4 Hz. Accordingly, only a single simulation study with limited geometry currently exists for TPS. We considered a high-resolution three-dimensional (3D) whole human head model in addition to water bath simulations. We anticipate that the results of this study will help researchers investigating LIFU have a better understanding of the effects of the two different techniques.

Approach: With an objective to first reproduce previous computational results, we considered two spherical tFUS transducers that were previously modeled. We assumed identical parameters (geometry, position, and imaging data set) to demonstrate differences, purely because of the waveform considered. For simulations with a 3D head data set, we also considered a parabolic transducer that has been used for TPS delivery.

Results: Our initial results successfully verified previous modeling workflow. The tFUS distribution was characterized by the typical elliptical profile, with its major axis perpendicular to the face of the transducer. The TPS distribution resembled two mirrored meniscus profiles, with its widest diameter oriented parallel to the face of the transducer. The observed intensity value differences were theoretical because the two waveforms differ in both intensity and time. The consideration of a realistic 3D human head model resulted in only a minor distortion of the two waveforms.

Significance: This study simulated TPS administration using a 3D realistic image-derived data set. Although our comparison results are strictly limited to the model parameters and assumptions made, we were able to elucidate some clear differences between the two approaches. We hope this initial study will pave the way for systematic comparison between the two approaches in the future.

Keywords: Human head model, low-intensity focused ultrasound, numerical simulation, transcranial focused ultrasound, transcranial pulse stimulation

Conflict of Interest: Soterix Medical distributes noninvasive neuromodulation devices, including transcranial pulse stimulation. The authors reported no other conflict of interest.

INTRODUCTION

Ultrasound has been used extensively in medicine and industry for more than 70 years.[1–4] Ultrasound as a technique for neuromodulation is essentially characterized into two main categories segregated by the intensity (spatial peak temporal average intensity [SPTA]) of the acoustic wave. High-intensity focused ultrasound (HIFU) with intensity typically >1 W/cm^2 produces

Address correspondence to: Dennis Q. Truong, PhD, Research and Development, Soterix Medical, 1480 US 9, Suite 204, Woodbridge Township, NJ 07095, USA. Email: dtruong@soterixmedical.com

[1] Research and Development, Soterix Medical, Woodbridge, NJ, USA;
[2] Research Program on Cognition and Neuromodulation Based Interventions, Department of Psychiatry, University of Michigan, Ann Arbor, MI, USA;
[3] Mental Health Service, VA Ann Arbor Healthcare System, Ann Arbor, MI, USA; and
[4] Department of Biomedical Engineering, The City College of New York, City University of New York, New York, NY, USA

reliable and permanent brain lesions through thermal ablation, whereas low-intensity focused ultrasound (LIFU) does not produce lesions but can excite or suppress neural activity with very rare occurrence of adverse effects.[5] Although HIFU secured the United States Food and Drug Administration's approval for essential tremor in 2016 and approval for other conditions is apparently on the horizon, efforts aimed at determining clinical utility for LIFU have only recently begun. Furthermore, LIFU can be subdivided into two techniques that use different waveforms but operate within the same ultrasound frequency range. Transcranial focused ultrasound (tFUS) characterized by long trains (several hundred milliseconds) has been shown to both potentiate and suppress neural activity as well as alter behavior in mammalian brains.[6]

The second technique, based on single ultrashort high-intensity ultrasound pulses (~3 µs) repeated every 200 to 300 ms, is referred to as transcranial pulse stimulation (TPS). TPS has recently demonstrated safety and efficacy in patients with Alzheimer disease.[7] Furthermore, in a follow-up study, TPS has been shown to reduce cortical atrophy in the same patients from the first study.[8] Although TPS uses a maximum peak pressure of up to 25 MPa, current application is limited by a finite number of pulses per treatment and characterized by a maximum SPTA intensity of 0.1 W/cm^2. This limitation serves as the maximum safe allowable dose based on the clinical data collected thus far.[7] Although the focusing performance of tFUS (ie, both spatial and depth focality) has been simulated by several groups,[9–17] the application of TPS has only been simulated using a restricted geometry based on computed tomography scans.[7] The main objective of this study was therefore to perform a numerical comparison of tFUS with TPS, using a highly detailed whole human head model in addition to free water simulations. This would facilitate a better understanding of the newly introduced TPS technique in relation to the more common tFUS approach and thereby guide rational design of experimental protocols.

It is to be noted that the aforementioned computational efforts to simulate tFUS have considerably varied in domain/geometry, equation modeling the ultrasound propagation, and complexity considered (based on the specific questions that the study aimed to address). To our knowledge, the study by Deffieux and Konofagou[9] was the first to evaluate tFUS with a focus on the blood-brain barrier (BBB) opening. They considered a three-dimensional (3D) primate and human geometry and investigated the focalization properties of single-element transducers across a range of low frequencies (300–1000 kHz). Pulkkinen et al[10] considered a fluid-solid model and then an angular spectrum method for propagation in the brain to compare simulations with actual phantom measurements. Legon et al[11,12] demonstrated ultrasound targeting ability by showing projections of measured acoustic fields onto a realistic human head model. The effect of heating and tissue properties were systematically studied for the first time by considering a 2D geometry with axial symmetry.[13] Robertson et al[14] considered a 2D geometry to investigate the impact of skull geometry and related parameters, whereas Tarnaud et al[16] explored the ultrasonic modulation of subthalamic nucleus by considering a model based on neurons specific to the region (the Otsuka model and the bilayer sonophore model). Samoudi et al[15] was the first study that considered a detailed 3D whole human head model and quantified focusing performance and energy deposition through a sensitivity analysis.

In this study, similar to Samoudi et al[15], we considered a full-wave finite-difference time-domain (FDTD) simulation platform to simulate both tFUS and TPS techniques and to investigate the corresponding acoustic intensity distribution. We first evaluated the intensity distribution in free water and then determined the same in an image-derived model. The Multimodal Imaging–based Detailed Anatomical data set, named "MIDA," was considered,[18] with a single-element focused transducer (SEFT) positioned at the side of the head. The same SEFT geometry and parameters used for free water validation by Samoudi et al[15] were used for both ultrasound techniques in this study. Likewise, the same SEFT geometry that was used for the MIDA model was repeated here. In addition, for the realistic head MIDA simulations, we considered the transducer design based on the device that delivers TPS. Samoudi et al[15] previously modeled a tFUS transducer in a water tank and validated the model with hydrophone data published by Mueller et al.[13] The water tank tFUS models were then extended to anatomically precise image-derived head models. Here, we extended the pipeline developed by Samoudi et al[15] to TPS waveforms.

MATERIALS AND METHODS

Waveform Parameters: Steady State vs Transient Considerations

The key difference in modeling tFUS vs TPS is the applied waveform. The ultrasound waveforms used in tFUS and TPS differ in shape, intensity, and timescale. tFUS commonly uses a constant frequency carrier wave delivered as repeated pulse trains, whereas TPS delivers a single high-pressure short-duration shockwave pulse that is then repeated. In keeping with previous tFUS modeling, the tFUS pulse was simulated as a sinusoid with a frequency and amplitude of 500 kHz and 0.145 MPa or 0.813 kPa ($P_0\sin(2\pi ft)$, where P_0=0.145 MPa or 0.813 kPa, f=500 kHz).[14] For TPS, a wavelet function was used to simulate the shape of the shockwave produced by the TPS transducer. The specific parameters of the wavelet were originally approximated to fit hydrophone measurements in models and experiments performed and provided by Storz Medical (Storz Medical AG, Tägerwilen, Switzerland).[7] The resulting waveform was simulated as a Gaussian weighted sine wavelet with an amplitude and duration of 2 MPa and 4 µs. The full equation is as follows: $P_0\, e^{-\left(\frac{t-\left(\frac{4}{f}\right)}{\sigma}\right)^2} \sin(2\pi ft)$, where $P_0 = 2$ MPa, $f = 250$ kHz, $\sigma = 2$ µs. Although the function was originally calibrated on a multipart model of a TPS transducer with a parabolic reflector and cylindrical emitter, herein, we modeled the geometry of the TPS transducers as simplified SEFTs. This was intentional, in keeping with the level of detail and related considerations in Samoudi et al[15] for the tFUS transducers.

These differences in tFUS and TPS waveforms affect the choice of simulation method. The transient time varying (as opposed to steady frequency) shape of the TPS shockwave necessitates a full-wave time-dependent method such as FDTD. This represents another specific consideration in modeling transient vs steady frequency pulses.

Ultrasound Propagation Model

A commercially available FDTD simulation platform was used in this study to model the two transcranial ultrasound–based techniques. Specifically, the acoustic physics module in Sim4Life (Sim4Life, Zurich, Switzerland) was used to apply the Westervelt-

Table 1. Acoustic Material Properties of Head Tissues.

Material	Speed of sound (m s^{-1})	Density (kg m^{-3})	Attenuation coefficient (Np m^{-1} MHz^{-1})	Nonlinearity parameter (B/A)
Skin/soft tissue	1624	1109	10.579	4.96*
Muscle	1588	1090	3.356	7.166
Blood	1578	1050	1.143	6.1125
Fat	1440	911	2.053	10.0712
Skull	2814	1908	27.2765	4.96*
CSF	1483	1000	0.025	4.96*
Air/sinus	343	1.16	0.00979	4.96*
Brain	1546	1046	2.76	6.7
Water	1482	994	0.0126642	4.96

*Estimated like water.

Lighthill equation $\left(\rho \nabla \cdot \frac{1}{\rho}\nabla p - \frac{1}{c^2}\frac{\partial^2 p}{\partial t^2} + \frac{\delta}{c^4}\frac{\partial^3 p}{\partial t^3} + \frac{\beta}{2\rho c^4}\frac{\partial^2 p^2}{\partial t^2} = 0\right)$ to a 3D FDTD method solver. The spatial distribution of pressure in the region of interest was solved as a function of transducer surface pressure. Transducer surface pressure was initially calibrated to published hydrophone data in the free water models for tFUS. As a proof of concept, TPS models were simulated with fixed waveform parameters across all trials, and thus, TPS results were normalized to the maximum intensity per trial. Perfectly matched layer boundary conditions were applied to the model truncations to remove boundary reflections.

To ensure numerical convergence in the TPS simulations, grid size was progressively refined, whereas the mean squared error of pressure as a function of time was calculated at the focal point. Convergence was considered adequate at a grid resolution of 1.5 MHz, resulting in a mean squared error of <10% to balance model size and accuracy.

Comparison of Ultrasound Propagation in a Water Tank

A previously validated SEFT was modeled as a point of reference.[13,15] The experimental transducer was geometrically focused, having a center frequency of 0.5 MHz, a diameter of 30 mm, and a focal length of 30 mm. In Sim4Life, the SEFT was parameterized as follows: medium speed of sound = 1483 m/s; curvature radius = 50 mm; and aperture width = 30 mm. The source amplitude was 0.145 MPa for the tFUS simulation and 2 MPa for the TPS simulation. Model geometry was held constant between simulation conditions.

Comparison of Ultrasound Propagation in a 3D Full Head Realistic Model

The ultrahigh-resolution (0.5 mm isotropic) MIDA head model (IT'IS Foundation, Zürich, Switzerland[18]) was loaded into an image processing and meshing software (Simpleware, Synopsys, Mountain View, CA) as image masks representing tissues of interest (skin, fat, muscle, blood, skull, air, cerebrospinal fluid [CSF], and brain), and any errors in continuity and anatomical details were manually corrected. Some anatomical regions of similar material composition were merged to a single compartment (eg, various brain lobes, skull, mandible, and teeth). Surface meshes were generated for each tissue and imported into the FDTD simulation platform (Sim4Life, ZMT Zurich MedTech AG, Zürich, Switzerland). The speed of sound, density, attenuation coefficient, and nonlinearity parameters were defined for each tissue from the IT'IS v4.0 material data base included within Sim4Life (Table 1). The Open Multi-Processing (OpenMP ARB, Beaverton, OR) solver was used on a workstation with the following specifications: 32 cores with 64 threads, 3.7 GHz base clock, 256 GB RAM, and 1 TB solid state drive storage.

Transducer geometry was modeled using the SEFT template within Sim4Life. SEFT curvature radius (120 mm) and aperture (100 mm) were selected based on previously simulated designs with known peak intensities for tFUS.[15] The same water layer thickness (20 mm) was maintained between the surface of the transducer and the temporal region of the head model. The source amplitude was 0.813 kPa for the tFUS simulation and 2 MPa for the TPS simulation. Model geometry was held constant between simulation conditions. A third transducer based on the first TPS study was modeled based on an experimentally validated design. The TPS transducer was modeled in Solidworks (Dassault Systèmes SE, Vélizy-Villacoublay, France) as a paraboloid with an aperture of 50 mm, 53 mm focal distance, and 3 mm height (Table 2).

Comparison/Analysis of tFUS and TPS Waveforms/Quantification

The resulting pressure and intensity distributions were compared. Instantaneous intensity was calculated at peak time as $p(t)^2/\rho c$, where $p(t)$ is the pressure, ρ is the density, and c is the speed of sound, for both ultrasound modalities owing to the TPS pulse being transient. Pulse average intensity was still calculated for tFUS as a point of reference to previous tFUS publications. The full width at half maximum (FWHM) at the temporal peak was calculated and measured for each simulation, and maximum pressure and instantaneous intensity were quantified (Table 3). We further

Table 2. Comparison of Reflector Parameters Used in the Study.

Parameter	Free water SEFT	MIDA SEFT	TPS parabolic
Aperture	30 mm	100 mm	50 mm
Curvature radius	50 mm	120 mm	—
Reflector height	2.3 mm (calculated)	10.9 mm (calculated)	3 mm (calculated)
Operating frequency	0.5 MHz	0.5 MHz	—
Parabolic focal distance	—	—	53 mm

Table 3. Simulation Results for tFUS.

Parameter	tFUS	Samoudi et al[15]	Delta	%Delta
Maximum pressure (free water) (kPa)	836	830	6	0.723
Maximum instantaneous intensity (free water) (kW/m^2)	474	Not reported (23.45 W/cm^2 average intensity)	—	—
Maximum pressure (MIDA) (kPa)	7.55	6.42	1.13	17.6
Maximum instantaneous intensity (MIDA) (W/m^2)	34.8	Not reported (15.1 W/m^2 average intensity)	—	—
Beam axis FWHM (free water) (mm)	27	28.96	1.96	6.77
Transverse axis FWHM (free water) (mm)	3.8	3.98	−0.18	−4.52
Beam axis FWHM (MIDA) (mm)	24	22.9	1.1	4.80
Transverse axis FWHM (MIDA) (mm)	3.75	3.06	0.69	22.5

Computational results from the existing study were compared with the previous study in terms of absolute (Delta) and percentage change (%Delta).

quantified the difference in predicted values to the previous study in absolute and percentage terms.

RESULTS

Simulation in Free Water

As alluded earlier in the text, we performed free water simulations for the two techniques using the same spherical transducer used in a previous study[15] (Fig. 1). For tFUS, we considered a steady frequency sinusoid with the same pressure amplitude (0.145 MPa) that was required to deliver a desired target intensity in the region of interest. For TPS, we considered a wavelet function shaped as a Gaussian weighted sine function (with pressure amplitude = 2 MPa) that approximated the shape of measurements taken using a hydrophone[7] (Fig.2b). The decision to use the same transducer along with position and imaging data set for both cases was intentional to elucidate the difference in acoustic intensity distributions, mainly because of the different waveform considered.

As expected and shown previously, for tFUS, the average and the instantaneous intensity distributions indicate an elliptical profile,

which is further emphasized by the FWHM profile (Fig. 2c). In contrast, by virtue of simulating a single ultrashort pulse, the corresponding intensity distribution for TPS resembles the profile of two mirrored positive menisci (based on terminology commonly used in lens physics), with the trailing profile being the smaller of the two. Furthermore, the widest axis of the TPS profile is aligned parallel to the transducer in the transverse plane (Fig. 2d), whereas the major axis of the tFUS elliptical profile is aligned with the beam axis perpendicular to the face of the transducer. Overall, the instantaneous profiles are typically characterized by multiple individual peaks (Fig. 2c,d1). In addition, for tFUS, the peak instantaneous intensity values are typically twice as high as the corresponding peak average induced intensity (474 kW/m^2 vs 232 kW/m^2). Note that in this comparison, the TPS simulations were taken at a single instant in time at the temporal peak, whereas both average and instantaneous results were calculated for tFUS. In Samoudi et al[15] and more broadly in the tFUS modeling literature, the carrier wave is often modeled as a steady frequency sinusoid for the duration of the simulation period. This, in tFUS, is a fair approximation, given the typical number of cycles per pulse. For example, Mueller et al[12,13] used a center frequency of 0.5 MHz with a pulse duration of 360 μs, resulting in 180 cycles per pulse. This allows for a steady-state analysis in the frequency domain of the resulting intensity fields caused by a single long pulse.

Simulation in a 3D Realistic Human Head Model

In addition to using the same spherical transducer used in the free water simulations, we considered the parabolic transducer based on the first TPS clinical study (Fig. 3). Furthermore, it is to be noted that the spherical transducer dimensions were different (120 mm curvature radius/100 mm aperture) from the free water study (53 mm curvature radius/30 mm aperture). The assumed input pressure for the tFUS simulation was substantially lower (0.813 kPa) than the free water and TPS transducers because it was based on the goal of achieving 100 W/m^2 average in free water.[14] This naturally explains the drop in the intensity values for the tFUS simulations (16.4–34.8 W/m^2), as depicted in Figure 3b, in comparison with the free water simulations (232–474 kW/m^2) in Figure 2c.

For TPS and when using the SEFT, we observed the same two mirrored meniscus profiles similar to the free water simulations (Fig. 3c). This effect was pronounced for the FWHM plot (Fig. 3c2). In addition, TPS resulted in approximately the same spatial peak location as tFUS (within 1 cm). When considering a differently shaped transducer (parabolic), however, the induced intensity profile essentially reduces to a single maxima as opposed to the
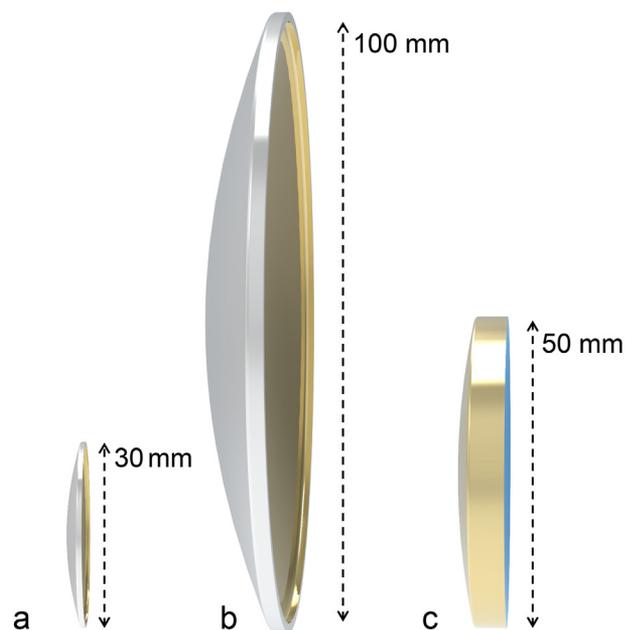
Figure 1. Transducer geometry considered. a. SEFT in free water. b. SEFT in MIDA-based model. c. Parabolic TPS transducer. [Color figure can be viewed at www.neuromodulationjournal.org]
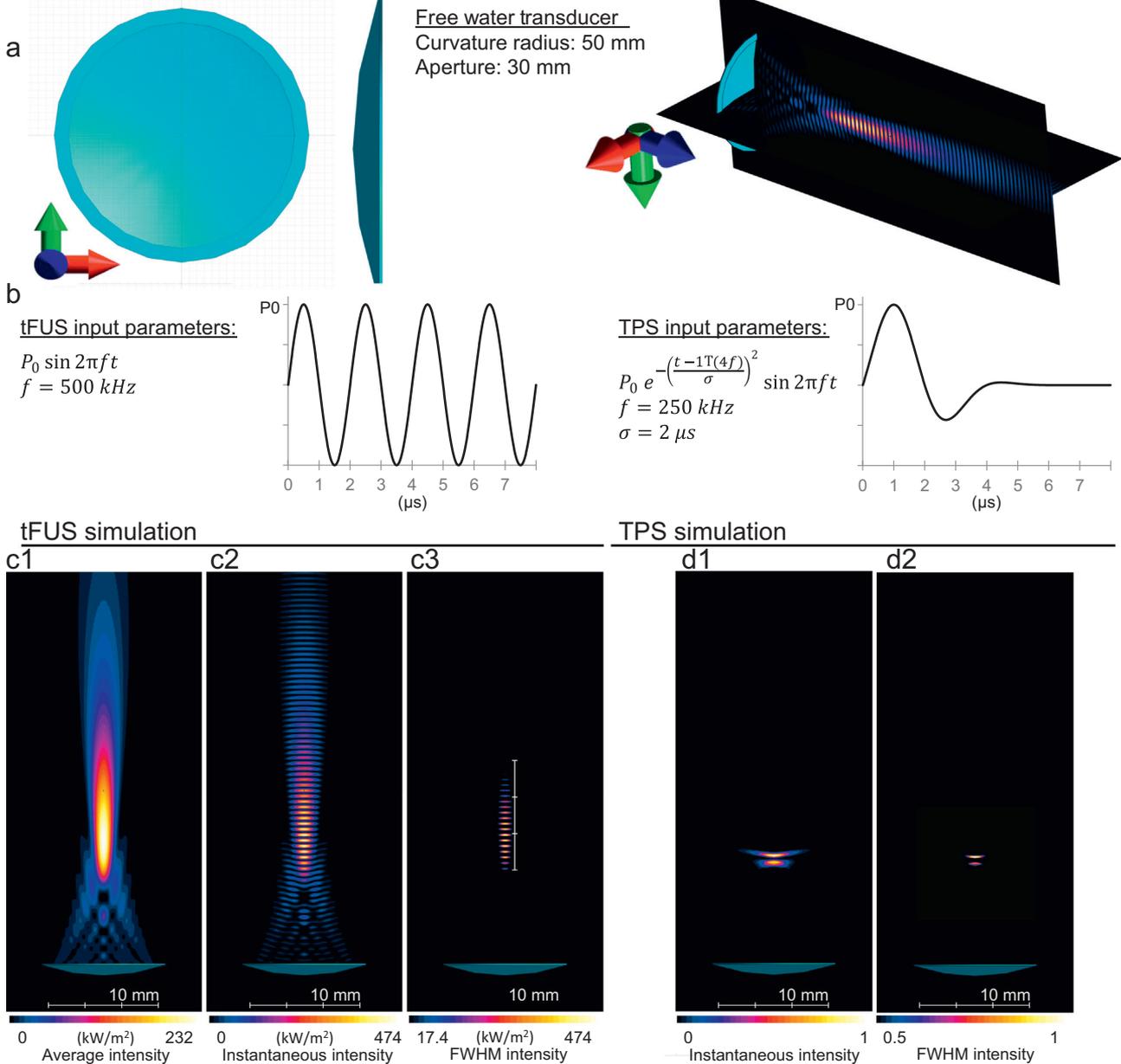
Figure 2. Free water simulations. 3D simulation of acoustic intensity sampled at the YZ plane through the focal point at the temporal peak. a. Both tFUS and TPS used the same spherical head model transducer. b. Parameters considered. c. tFUS intensity distributions in the YZ plane (c1: average; c2: instantaneous; c3: FWHM). d. TPS intensity distributions in the YZ plane (d1: instantaneous; d2: FWHM). Because TPS was simulated using a theoretical spherical transducer while using a driving function originally calibrated on its default transducer, TPS intensity plots are normalized. The TPS data therefore only illustrate spatial profile. [Color figure can be viewed at www.neuromodulationjournal.org]

spherical SEFT (Fig. 3d). Given the assumed transducer specification (Table 2), simulations confirmed a shorter focal length (~53 mm) when considering a realistic head geometry.

Overall, the profiles of both approaches (tFUS and TPS) stayed elliptic and meniscus-like, respectively, in the 3D head model, similar with the free water simulations. Furthermore, the profile orientations with respect to the face of the transducer (perpendicular for tFUS and parallel for TPS) remained the same. This confirmed the notion that consideration of head tissues does not affect the overall distribution (profile and orientation). However,

looking closely, we observed minute distortions in the induced profiles, for instance, uneven peak distribution within the ellipse for tFUS (Fig. 3b3).

The quantification of the FWHM profile in free water simulation for tFUS confirms previous findings (Table 3).[15] We note a maximum deviation of 6.77% in free water simulations (beam axis FWHM) and 22.54% in realistic 3D model simulations (transverse axis FWHM). This is expected, given the MIDA models differed slightly in tissues modeled and transducer placement, whereas the free water simulations considered identical parameters and
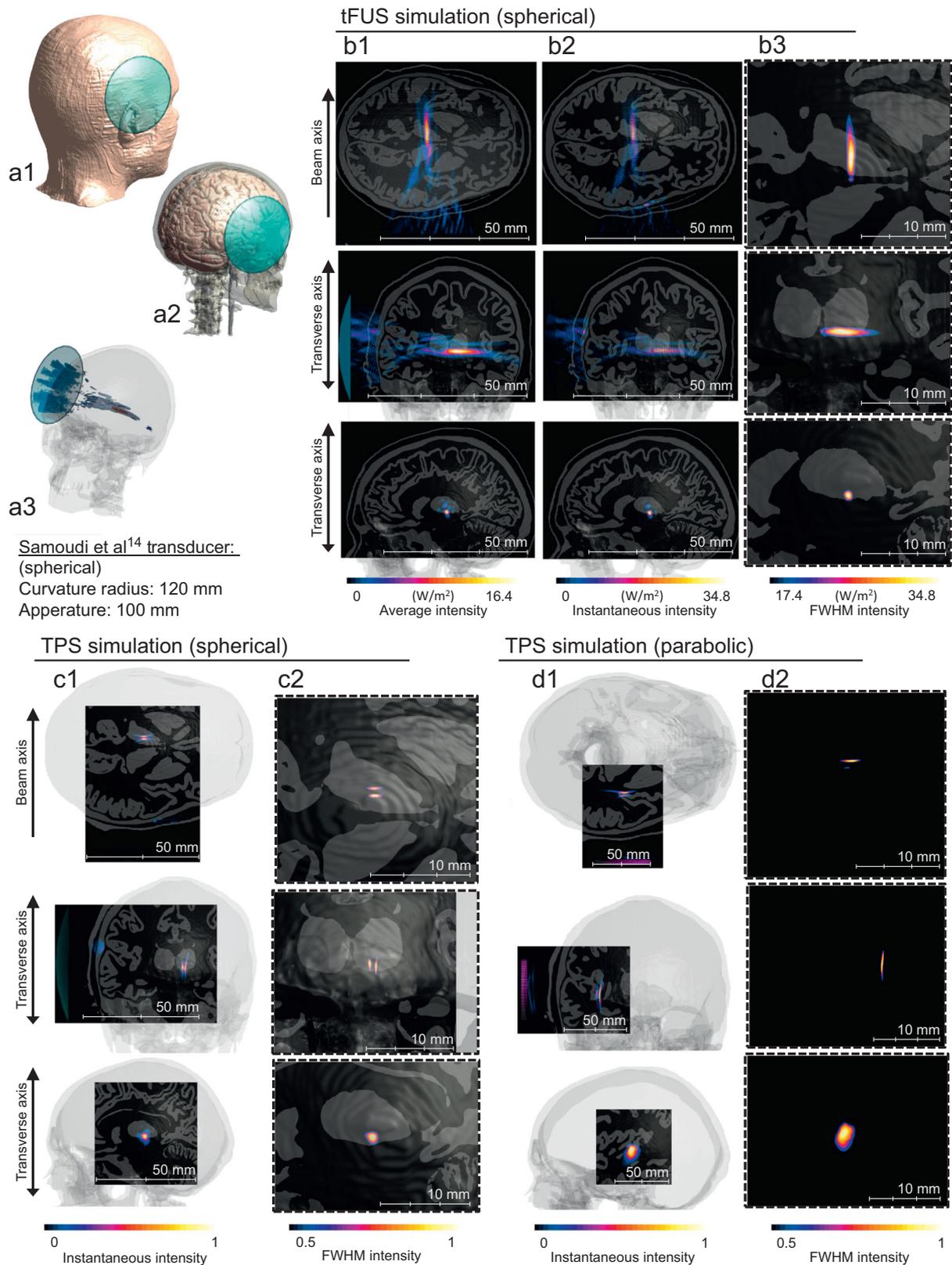
Figure 3. Realistic head (MIDA model) simulations. a1. Transducer location with respect to the MIDA-based model. a2. The scalp and skull tissues are made semitransparent to reveal underlying brain tissue. a3. Beam profile for tFUS. b. Axial, coronal, and sagittal view of tFUS intensity (b1: average; b2: instantaneous; b3: FWHM). c. TPS simulation using the same spherical SEFT used in tFUS (c1: instantaneous; c2: FWHM). d. TPS simulation using transducer specific to its delivery (d1: instantaneous; D2: FWHM). Similar to the free water simulations, TPS plots are normalized because the driving function used was originally calibrated on a more complex multipart model of a specific size transducer. The TPS data therefore only illustrate spatial and depth profile. Representative cross-section plots included here correspond to the location of maximum induced intensity. [Color figure can be viewed at www.neuromodulationjournal.org]

Table 4. Simulation Results for TPS.

Parameter	TPS SEFT	TPS parabolic transducer
Beam axis FWHM (free water)	3 mm	—
Transverse axis FWHM (free water)	6 mm	—
Beam axis FWHM (MIDA)	3 mm	3.5 mm
Transverse axis FWHM (MIDA)	7 mm	11 mm

geometry. In free water, the tFUS beam axis was approximately 6× the transverse axis, whereas the TPS transverse axis was approximately 2× the beam axis (Table 4). This is likely attributed to the inherent properties of the tFUS and TPS waveforms, particularly the much shorter pulse duration of the latter. This pattern was consistent when a realistic 3D head model was considered.

DISCUSSION

LIFU has gained tremendous, increasing interest in the past two decades for neuromodulation research.[3,17–19] As opposed to HIFU, the basic motivation behind LIFU techniques is that LIFU uses low energy levels to modulate desired brain regions focally and reversibly without opening of the BBB and without generating morphological changes within the brain. Although the exact mechanism for neuromodulation is the subject of ongoing investigation, it is theorized that acoustic stimulation can change effective membrane or membrane channel properties that, in turn, affect membrane potential.[20–23] The influence of mechanical vs thermal mechanisms of acoustic stimulation is debated, but it could be a differentiating factor between tFUS and TPS.[24–27] Future studies could investigate this directly. With respect to model interpretation, the consideration of intensity as a proxy for neuromodulation is rational because it indicates regions in the brain directly affected by ultrasound stimulation. Intensity (power per unit area) is proportional to pressure squared and commonly used in ultrasound stimulation modeling.[5,7,15,22]

The commonly used approach (tFUS) uses pressure applied at center frequencies in the 200 to 650 kHz range. The pressure stimulus over time resembles a burst of waves with duration in the millisecond range, followed by an inactive period.[5] Sonication time, which is referred to as a train of these repeated bursts and corresponding inactive periods, extends for several minutes. In contrast to tFUS, TPS uses single ultrashort pulses (3 µs) repeated at 4 Hz with a similar sonication time of several minutes. Because a multitude of tFUS simulations have already been performed, our goal was to primarily extend a recently developed computational framework for tFUS to TPS waveforms. The eventual motivation was to facilitate a better understanding of the TPS technique in relation to tFUS. We considered both water bath and realistic 3D human head models.

We considered two tFUS transducers previously modeled in Samoudi et al[15] to serve as points of comparisons between the two techniques. Although the model parameters were nearly identical (transducer geometry, transducer position, waveform, imaging data set), in keeping with an initial objective to reproduce these previous results, updates were applied to the anatomical model. Our version of the MIDA-based model included segmentation for the skin, fat, muscle, and CSF, whereas the skull mask was merged into one. Nonetheless, the resulting average intensities in the MIDA model were comparable (15.1 W/m² vs 16.4 W/m² in Samoudi et al[15] and Fig. 3b, respectively). The skull tissue remains the primary barrier for ultrasound delivery, and a realistic depiction is important; however, our results imply that the consideration of a single homogenous skull tissue does not substantially affect the induced intensity value in comparison with using a layered tissue.

Our computational results confirm the elliptical profile of the induced acoustic distribution for tFUS. This directly reflects the typical assumed pulse duration for tFUS extending to several hundred cycles. In contrast, the mirrored positive meniscus profile shape for TPS was the result of a single transient pulse observed at the time point considered (ie, the temporal peak). As a result, the widest axis for the TPS profile was aligned parallel to the face of the transducer in the transverse plane as opposed to the beam axis alignment for tFUS. We can, however, expect the TPS profile to elongate along the beam axis if considering a temporal average, which would then resemble the tFUS profile at least in major axis alignment.[7] Because ultrasound stimulation and dosing are a function of several parameters from the ultrasound transducer, its primary frequency, pressure (amplitude), placement, and cranium coupling, our results are naturally limited to the parameters considered and assumptions made. Nonetheless, we were able to demonstrate some key differences related to profile shape and orientation between the two approaches that are expected to hold under different parameters. Furthermore, our results confirm previous work demonstrating that a simple SEFT has the potential to deliver ultrasonic energy to deeper subcortical structures. The induced profile for the TPS parabolic transducer was shallower but a direct result of the shorter focal distance considered. Therefore, irrespective of the choice of the ultrasound technique considered, the ability to target deeper structures can be maintained.

As alluded earlier in the text, our work is limited by the consideration of FWHM shape only at peak time for TPS simulation. Although the temporal average peak should be at the temporal peak as depicted in Figure 3c,d, the actual pressure wavefront is dynamic, and it passes other structures before reaching the spatial peak location. An extensive analysis would ideally involve multiple time points, but the computational demand of such an analysis is steep. Therefore, future work would require additional investment in workstation disk storage and swap space. With regard to distortion between free water and the human head model, we observed minimal difference. However, this analysis was limited to one transducer location aimed perpendicular to the skull. Other locations and angles remain to be tested with TPS to determine whether the same observation would continue to hold. In fact, because studies based on tFUS suggest greater distortion, and attenuation can occur at more skewed angles,[28] it would be reasonable to expect the same with TPS.

Computational approaches such as these have continued to fundamentally affect a wide range of brain stimulation modalities over the years, from optimizing delivery to performing safety analysis.[29–34] Furthermore, these predictions have helped in elucidating stimulation profiles, understanding mechanism of action, correcting adoption, retrospectively explaining stimulation outcome, and thereby advancing stimulation administration in general. We expect this initial study to guide researchers interested in exploring ultrasound-based brain stimulation techniques by providing a better understanding of the differences and similarities between the two aforementioned approaches. This, in turn, would spur experimentation, validation, additional modeling-related questions, technology advancements, and more.

Acknowledgements

Authorship Statements

Dennis Q. Truong, Abhishek Datta, and Chris Thomas designed and conducted the study, including data collection and data analysis. Dennis Q. Truong and Abhishek Datta prepared the manuscript draft, with important intellectual input from Benjamin M. Hampstead. Abhishek Datta provided funding for the study and for editorial support. Dennis Q. Truong, Abhishek Datta, and Chris Thomas had complete access to the study data. All authors approved the final manuscript.

How to Cite This Article

REFERENCES

1. Rezayat E, Toostani IG. A review on brain stimulation using low intensity focused ultrasound. *Basic Clin Neurosci*. 2016;7:187–194.
2. Darrow DP. Focused ultrasound for neuromodulation. *Neurotherapeutics*. 2019;16:88–99.
3. Meng Y, Hynynen K, Lipsman N. Applications of focused ultrasound in the brain: from thermoablation to drug delivery. *Nat Rev Neurol*. 2021;17:7–22. https://doi.org/10.1038/s41582-020-00418-z.
4. Fry FJ, Ades HW, Fry WJ. Production of reversible changes in the central nervous system by ultrasound. *Science*. 1958;127:83–84.
5. Pasquinelli C, Hanson LG, Siebner HR, Lee HJ, Thielscher A. Safety of transcranial focused ultrasound stimulation: a systematic review of the state of knowledge from both human and animal studies. *Brain Stimul*. 2019;12:1367–1380. https://doi.org/10.1016/j.brs.2019.07.024.
6. Fomenko A, Neudorfer C, Dallapiazza RF, Kalia SK, Lozano AM. Low-intensity ultrasound neuromodulation: an overview of mechanisms and emerging human applications. *Brain Stimul*. 2018;11:1209–1217.
7. Beisteiner R, Matt E, Fan C, et al. Transcranial pulse stimulation with ultrasound in Alzheimer's disease—a new navigated focal brain therapy. *Adv Sci (Weinh)*. 2020;7:1902583. https://doi.org/10.1002/advs.201902583.
8. Popescu T, Pernet C, Beisteiner R. Transcranial ultrasound pulse stimulation reduces cortical atrophy in Alzheimer's patients: a follow-up study. *Alzheimers Dement (N Y)*. 2021;7:e12121. https://doi.org/10.1002/trc2.12121.
9. Deffieux T, Konofagou EE. Numerical study of a simple transcranial focused ultrasound system applied to blood-brain barrier opening. *IEEE Trans Ultrason Ferroelectr Freq Control*. 2010;57:2637–2653. https://doi.org/10.1109/TUFFC.2010.1738.
10. Pulkkinen A, Huang Y, Song J, Hynynen K. Simulations and measurements of transcranial low-frequency ultrasound therapy: skull-base heating and effective area of treatment. *Phys Med Biol*. 2011;56:4661–4683.
11. Legon W, Sato TF, Opitz A, et al. Transcranial focused ultrasound modulates the activity of primary somatosensory cortex in humans. *Nat Neurosci*. 2014;17:322–329. https://doi.org/10.1038/nn.3620.
12. Mueller J, Legon W, Opitz A, Sato TF, Tyler WJ. Transcranial focused ultrasound modulates intrinsic and evoked EEG dynamics. *Brain Stimul*. 2014;7:900–908. https://doi.org/10.1016/j.brs.2014.08.008.
13. Mueller JK, Ai L, Bansal P, Legon W. Computational exploration of wave propagation and heating from transcranial focused ultrasound for neuromodulation. *J Neural Eng*. 2016;13:056002. https://doi.org/10.1088/1741-2560/13/5/056002.
14. Robertson JLB, Cox BT, Jaros J, Treeby BE. Accurate simulation of transcranial ultrasound propagation for ultrasonic neuromodulation and stimulation. *J Acoust Soc Am*. 2017;141:1726. https://doi.org/10.1121/1.4976339.
15. Samoudi MA, Van Renterghem T, Botteldooren D. Computational modeling of a single-element transcranial focused ultrasound transducer for subthalamic nucleus stimulation. *J Neural Eng*. 2019;16:026015. https://doi.org/10.1088/1741-2552/aafa38.
16. Tarnaud T, Joseph W, Martens L, Van Renterghem T, Tanghe E. Interaction of electrical and ultrasonic neuromodulation: a computational study. *Brain Stimul*. 2019;12:563. https://doi.org/10.1016/j.brs.2018.12.864.
17. Wojcik G, Mould J, Abboud N, Ostromogilsky M, Vaughan D. Nonlinear modeling of therapeutic ultrasound. In: Souheil H, Watkin KL, eds. *1995 IEEE Ultrasonics Symposium Proceedings. An International Symposium*. Vol. 2. IEEE; 1995:1617–1622.
18. Iacono MI, Neufeld E, Akinnagbe E, et al. MIDA: a multimodal imaging–based detailed anatomical model of the human head and neck. *PLoS One*. 2015;10: e0124126. https://doi.org/10.1371/journal.pone.0124126.
19. Bystritsky A, Korb AS, Douglas PK, et al. A review of low-intensity focused ultrasound pulsation. *Brain Stimul*. 2011;4:125–136.
20. Tyler WJ. The mechanobiology of brain function. *Nat Rev Neurosci*. 2012;13:867–878.
21. Plaksin M, Kimmel E, Shoham S. Cell-type-selective effects of intramembrane cavitation as a unifying theoretical framework for ultrasonic neuromodulation. *eNeuro*. 2016;3:ENEURO.0136-15.2016.
22. di Biase L, Falato E, Di Lazzaro V. Transcranial focused ultrasound (tFUS) and transcranial unfocused ultrasound (tUS) neuromodulation: from theoretical principles to stimulation practices. *Front Neurol*. 2019;10:549. https://doi.org/10.3389/fneur.2019.00549.
23. Kamimura HAS, Conti A, Toschi N, Konofagou EE. Ultrasound neuromodulation: mechanisms and the potential of multimodal stimulation for neuronal function assessment. *Front Phys*. 2020;8:150. https://doi.org/10.3389/fphy.2020.00150.
24. Collins MN, Legon W, Mesce KA. The inhibitory thermal effects of focused ultrasound on an identified, single motoneuron. *eNeuro*. 2021;8:ENEURO.0514-20.2021. https://doi.org/10.1523/ENEURO.0514-20.2021.
25. d'Agostino MC, Craig K, Tibalt E, Respizzi S. Shock wave as biological therapeutic tool: From mechanical stimulation to recovery and healing, through mechanotransduction. *Int J Surg*. 2015;24:147–153.
26. Kubanek J, Shukla P, Das A, Baccus SA, Goodman MB. Ultrasound elicits behavioral responses through mechanical effects on neurons and ion channels in a simple nervous system. *J Neurosci*. 2018;38:3081–3091. https://doi.org/10.1523/JNEUROSCI.1458-17.2018.
27. Lohse-Busch H, Reime U, Falland R. Symptomatic treatment of unresponsive wakefulness syndrome with transcranially focused extracorporeal shock waves. *NeuroRehabilitation*. 2014;35(2):235–244. https://doi.org/10.3233/NRE-141115.
28. Park TY, Pahk KJ, Kim H. Method to optimize the placement of a single-element transducer for transcranial focused ultrasound. *Comput Methods Programs Biomed*. 2019;179:104982. https://doi.org/10.1016/j.cmpb.2019.104982.
29. Butson CR, McIntyre CC. Role of electrode design on the volume of tissue activated during deep brain stimulation. *J Neural Eng*. 2006;3:1–8. https://doi.org/10.1088/1741-2560/3/1/001.
30. Deng ZD, Lisanby SH, Peterchev AV. Electric field depth-focality tradeoff in transcranial magnetic stimulation: simulation comparison of 50 coil designs. *Brain Stimul*. 2013;6:1–13. https://doi.org/10.1016/j.brs.2012.02.005.
31. Datta A, Bansal V, Diaz J, Patel J, Reato D, Bikson M. Gyri-precise head model of transcranial direct current stimulation: improved spatial focality using a ring electrode versus conventional rectangular pad. *Brain Stimul*. 2009;2:201–207, 207.e1.
32. Roth Y, Amir A, Levkovitz Y, Zangen A. Three-dimensional distribution of the electric field induced in the brain by transcranial magnetic stimulation using figure-8 and deep H-coils. *J Clin Neurophysiol*. 2007;24:31–38.
33. Haberbosch L, Datta A, Thomas C, et al. Safety aspects, tolerability and modeling of retinofugal alternating current stimulation. *Front Neurosci*. 2019;13:783.
34. Lempka SF, McIntyre CC. Theoretical analysis of the local field potential in deep brain stimulation applications. *PLoS One*. 2013;8:e59839.

COMMENTS

The article compares simulation results of applying TPS and tFUS to a 3D human head model. This study is well written and clear, and it provides some information regarding the differences between tFUS and TPS using certain stimulation parameters. A more comprehensive study is required to compare the differences between the two techniques using different stimulation parameters and determine the sensitivity of each technique to different assumptions used in the model.

Atefeh Ghazavi, MS
Durham, NC, USA

613